Self-tuned Adaptation Rate Lyapunov based Voltage Controller for a Grid Connected PV System

Malay Bhunia
Department of Electrical Engineering
National Institute of Technology Rourkela
Odisha 769008, India
malay321@gmail.com

Bidyadhar Subudhi
School of Electrical Sciences
Indian Institute of Technology Goa
Goa 403401, India
bidyadhar@iitgoa.ac.in

Pravat Kumar Ray
Department of Electrical Engineering
National Institute of Technology Rourkela
Odisha 769008, India
rayp@nitrkl.ac.in

***Abstract*—This paper proposes a novel Self-tuned Adaptation gain enable Lyapunov Based Adaptive Controller (STLBAC) for three-phase Grid-Tied PV System (GTPVS). There are numbers of influencing factors for achieving PV voltages tracking such as intermittent solar irradiance, aging of DC link capacitor. To accomplish better performance of GTPVS in presence of uncertainties in irradiance and DC-link capacitor, a STLBAC is proposed to regulate the PV panel voltage. An adaptation mechanism is designed by using Lyapunov theory to adjust gains such that the desired PV voltage tracking response can be achieved despite the uncertainties. The performances of the proposed STLBAC are verified by using simulation and experimentation on a 2 kW GTPVS. The efficacy of the proposed STLBAC has been compared with Robust Nonlinear Adaptive Backsteeping Controller (RNBC). It is found that the STLBAC provides better PV voltage tracking with less voltage ripple. Also, the grid current THD yielded by STLBAC is less as compared to RNBC. The PV voltage tracking found critically damped with desired settling time (i.e., 20 ms). The grid currents and grid voltages Total Harmonics Distortion (THD) are found as 2.1 % and 2 % respectively which are within the limit of IEEE-1547 standard.**

***Index Terms*—Adaptive control, Lyapunov, PV system, Self-tuned adaptation gain.**

I. Introduction

CONTROL problem related with PV system is difficult because of the nonlinear and environment dependent PV panel characteristics. Further, performances of Grid-Tied PV System (GTPVS) degrade with time due to aging associated problems in GTPVS [1]. The parameters of DC-link capacitor change with operating time due to aging [2]. The inductance and resistance of the interfacing filter change because of operating conditions [3].

Thus parametric uncertainties, associated with DC-link capacitor and interfacing filter, affect in overall performance of GTPVS. Some reported advanced controllers, such as Model Predictive Controller (MPC) [4], integral sliding mode controller [5], and adaptive backstepping controller [6], are employed to achieve the robust tracking performances of grid current despite the uncertainties in coupling filter.

A cascaded control structure, in Synchronous Rotating Frame, is generally employed for achieving accurate tracking performances of GTPVS. In cascaded control structure, the PV Voltage Controller (PVVC) loop is in outer loop, and Grid Current Controllers (GCCs) are in their inner loop [7]. The MPPT algorithm searches the reference operating voltage (V_{ref}) of PV modules through continuous iteration process. The PVVC provides tracking of V_{ref}, and simultaneously generation of grid current reference for GCC. Voltage tracking performance of PVVC is affected by DC-link capacitor due to aging in it [2]. The grid current THD becomes more than 5 % at low irradiance [8]. The ripple in PV voltage causes the fluctuation in grid current reference. This further affects the steady state responses of GCC. Thus, tracking performance PVVC plays an important in over all grid power quality.

The literature survey suggests that aging in DC-link capacitor plays an important role in achieving improved performances of GTPVS. A Robust Nonlinear Adaptive Backstepping Controller (RNBC) has been designed for GTPVS in [9] to achieve the robust tracking performance under the parametric uncertainties of DC-link capacitor of GTPVS. However, RNBC causes the high chattering in final control action of GTPVS. Hence, PV voltage ripple increases, and simultaneously affects in the THD of grid current. In view of the above, a Lyapunov Based Adaptive Controller (LBAC) to control the PV voltage (V_{pv}) of the GTPVS is developed [10]. The LBAC provides the improved performances of GTPVS under the uncertainties in irradiance and DC-link capacitor. The adaptation gain of LBAC plays an important role in achieving the improved performance. In aforesaid LBAC, the optimal adaptation gain is chosen by hit and trial method though simulation studies, which is rigorous and time consuming method. In view of the above difficulty in selection of adaptation rate of LBAC, we have proposed a Self-Tuned adaptation rate based LBAC (STLBAC) for controlling the PV voltage of single stage GTPVS. The novelty of this work is to design an auto-tuned adaptation mechanism for the LBAC [10] such that following improved performances of GTPVS can be achieved in GTPVS.

1) critically damped response in PV voltage (V_{pv}) tracking with low voltage ripple in face of aging in DC-link capacitor.
2) ensuring superior grid current THDs under uncertainties in

irradiance.

The paper is organized as follows. Section II presents modeling of GTPVS. Section III presents the formulation of STLBAC for GTPVS. The efficacy of the proposed STLBAC based PVVC has been discussed in Section IV. Finally, the conclusions are drawn in Section V.

II. Modeling of GTPVS

The diagram of a GTPVS is shown in Fig. 1. The PV module current and voltage are denoted by I_{pv} and V_{pv} respectively. L and R denote the respectively inductance and resistance of the coupling filter. C define capacitance of DC-link capacitor. $e_{a,b,c}$ are the PCC voltages. $i_{a,b,c}$ denote the grid currents. $S_{a,b,c}$ represent the modulating signals of GTPVS. The $S_{1,2,..6}$ denote the different switching signals of the GTPVS.

The state space model of the GTPVS can be obtained form Fig. 1 as [10] [11]:

$$\begin{aligned} L\frac{di_a}{dt} &= \frac{1}{3}V_{pv}\left(2S_1 - S_3 - S_5\right) - i_a R - e_a \\ L\frac{di_b}{dt} &= \frac{1}{3}V_{pv}\left(2S_3 - S_1 - S_5\right) - i_b R - e_b \\ L\frac{di_c}{dt} &= \frac{1}{3}V_{pv}\left(2S_5 - S_1 - S_3\right) - i_c R - e_c \\ C\frac{dV_{pv}}{dt} &= I_{pv} - i_a S_1 - i_b S_3 - i_c S_5 \end{aligned} \tag{1}$$

The time invariant model of GTPVS in synchronous rotating frame (i.e., dq frame) can be obtained by applying the Park's transformation [11] to (1) as:

$$\left.\begin{aligned} L\frac{dI_d}{dt} &= -RI_d + V_{rd}; \quad L\frac{dI_q}{dt} = -RI_q + V_{rq} \\ \dot{V}_{pv} &= \frac{1}{C}i_{pv} - \frac{3}{2}\frac{I_d}{C}S_d - \frac{3}{2}\frac{I_q}{C}S_q \end{aligned}\right\} \tag{2}$$

where, $I_{dq0} = T_{abc}^{dq0} i_{abc}$, $E_{dq0} = T_{abc}^{dq0} e_{abc}$, and $S_{dq0} = T_{abc}^{dq0} S_{a,b,c}$, $V_{rd} = -L\omega I_q - E_d + V_{pv}S_d$, $V_{rq} = L\omega I_d - E_q + V_{pv}S_q$, T_{abc}^{dq0} is Park's transformation matrix [11], and I_d and I_q denote respectively direct and quadrature axis component of grid current.

III. Design of STLBAC for GTPVS

The proposed STLBAC for GTPVS is shown in Fig.1. In this STLBAC, V_{pv} is controlled by regulating the active power flow to the PCC. The active power is controlled by I_q, and the reactive power is controlled by I_d. The transfer function (G_{pv}(s)), for controlling V_{pv}, can be obtained from last equation of (2) as

$$G_{pv}(s) \equiv \left.\frac{V_{pv}(s)}{F_{pv}(s)}\right|_{I_d=0} = \frac{1}{sC} \tag{3}$$

where, we denotes F_{pv}=i_{pv}-$\frac{3}{2}I_q S_q$.

The desired Tracking Response (DTR) of PVVC is governed by V_{pvm} as

$$\frac{dV_{pvm}}{dt} = -a_m V_{pvm} + b_m V_{ref} \tag{4}$$

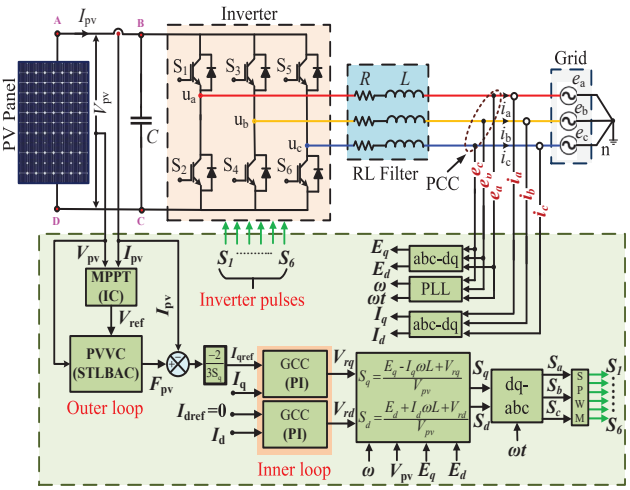

Fig. 1. A single stage GTPVS with adaptive PV voltage controller.

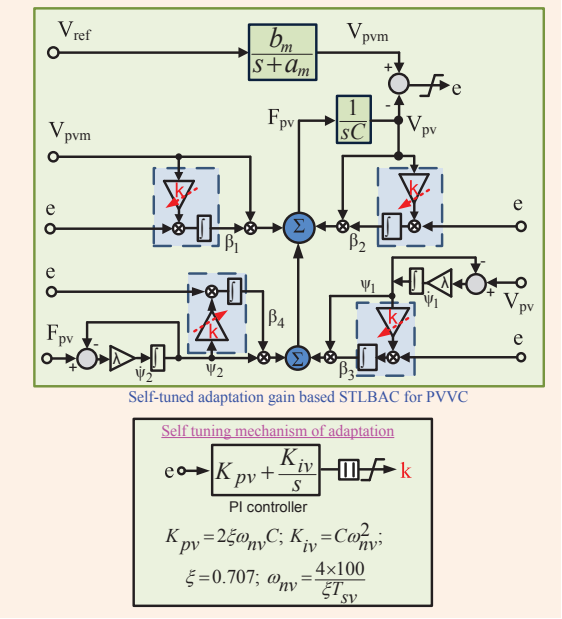

Fig. 2. Structure of the proposed STLBAC based PVVC.

where, $a_m(>0)$ and $b_m(>0)$ define the tracking characteristics of V_{pv} tracking. The proposed control law for V_{pv} tracking is chosen as

$$F_{pv} = \beta_1 V_{ref} + \beta_2 V_{pv} + \beta_3 \psi_1 + \beta_4 \psi_2 \tag{5}$$

where, β_1, β_2, β_3, and β_4 are the adaptation parameters; $\psi_1 = \frac{\lambda}{s+\lambda}V_{pv}$; $\psi_2 = \frac{\lambda}{s+\lambda}F_{pv}(s)$; $\frac{\lambda}{s+\lambda}$ is a low pass filter with $\lambda > 0$. On substitution of (5) into (3), the PV voltage dynamics can be obtained as:

$$\frac{dV_{pv}}{dt} = \frac{1}{C}\left(\beta_1 V_{ref} + \beta_2 V_{pv} + \beta_3 \psi_1 + \beta_4 \psi_2\right) \tag{6}$$

Define the error as e and time derivative of e as:

$$e = V_{pvm} - V_{pv}; \quad \dot{e}(t) = \dot{V}_{pvm} - \dot{V}_{pv} \tag{7}$$

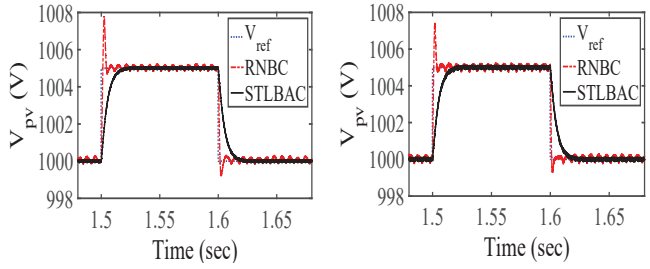

(a) (b)

Fig. 3. Step responses of V_{pv} tracking under different DC-link capacitor: (a) C=1.1 mF and (b) C=0.7 mF.

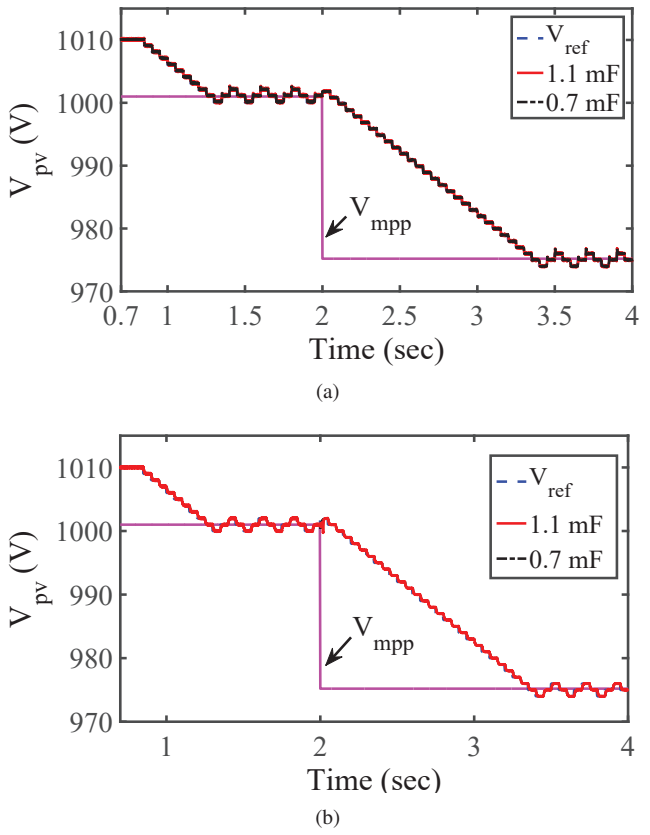

(a)

(b)

Fig. 4. Tracking of V_{pv} under different irradiance and under different C. Obtained with: (a) RNBC and (b) STLBAC.

As discussed in [10], the adaptation laws for the controller gains of the STLBAC can be obtained as:

$$\dot{\beta}_1 = keV_{ref}; \dot{\beta}_2 = keV_{pv}; \dot{\beta}_3 = \psi_1 ek; \dot{\beta}_4 = \psi_2 ek \quad (8)$$

The adaptation gain (k) plays a vital role in achieving the improved performance of adaptive controller. The high value of k increases the adaptation rate but causes high frequency oscillations response. Further, low value of k causes the continuous low frequency sustain oscillations in response. Thus, the optimal value of k should be selected so that the tracking is reasonable fast with less oscillation.The conventional hit and trial method is employed to find k in [10]. In our work,

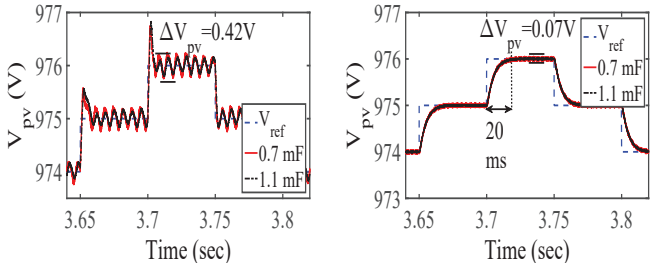

(a) (b)

Fig. 5. Zoomed view of V_{pv} tracking in Fig. 4 at 400 W/m^2; obtained with (a) RNBC and (b) STLBAC.

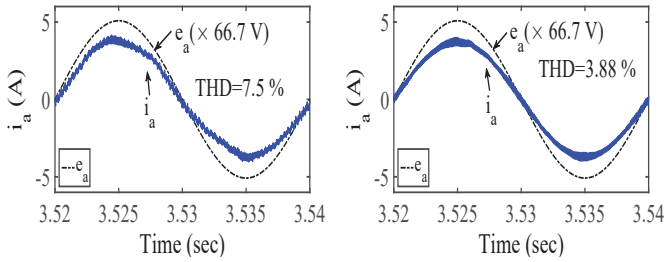

(a) (b)

Fig. 6. Grid current (i_a) at 400 W/m^2 with C=1.1 mF; obtained with: (a) RNBC and (b) STLBAC.

TABLE I
PARAMETERS OF GTPVS

Variable	Value	Variable	Value
R, L	0.1 Ω, 12 mH	MPPT sampling (T_{mppt})	0.05 sec
C	1.1 mF	MPPT step size (ΔV)	1 V
$e_{a,b,c}$	415 V, 50 Hz	Switching frequency (f_{sw})	10 kHz
T_{sv}, T_{si}	20 ms, 1 ms		

the adaptation gain (k) is tuned online through a PI controller where the V_{pv} tracking error (e) is taken as input to this PI controller. The output of this PI controller is passed through an absolute function before being used in controller as shown in Fig. 2. The settling time of the PI based adaptation mechanism is chosen as 100 times of the settling time of the PVVC. The K_{pv} and K_{iv} of PI based adaptation mechanism is calculated based on the nominal value of DC-link capacitor (C) as shown in Fig.2. The structure of proposed STLBAC based PVVC is shown in Fig.2. The desired settling time (T_{sv}) of critically damped V_{pv} tracking response is obtained by calculating a_m and b_m as a_m=b_m=$\frac{4}{T_{sv}}$.

The gains of PI controller (i.e., K_p and K_i) based GCC are found as [7]

$$K_p = 2\xi\omega_{ni}L - R; \; K_i = L\omega_{ni}^2; \; \omega_{ni} = \frac{4}{\xi T_{si}} \quad (9)$$

where, ξ=0.707 is the damping ratio, and $T_{si}$is settling time of GCC.

IV. RESULTS AND DISCUSSION

The proposed STLBAC based PVVC, as discussed in Section III, is verified through simulation studies in MAT-

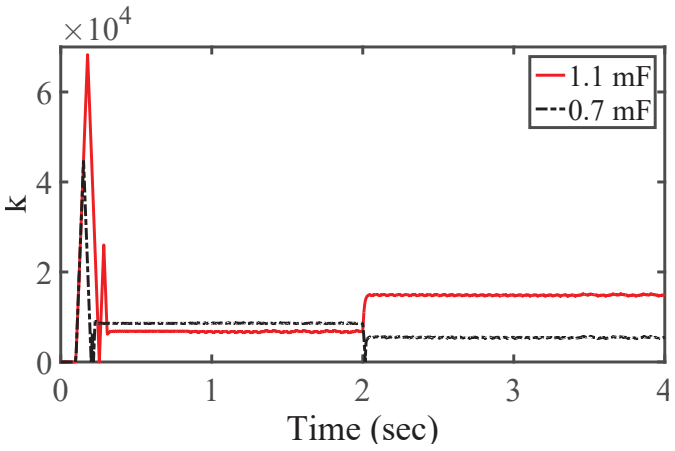

Fig. 7. Behavior of adaptation gain under different C.

TABLE II
CHARACTERISTICS OF PV ARRAY AT DIFFERENT IRRADIANCE

Irradiance (W/m^2)	V_{mpp} (V)	I_{mpp} (A)	P_{mpp} (W)
1000	1001	5	5005
400	975.2	1.981	1931.78

TABLE III
GRID CURRENT THDS OBTAINED WITH RNBC AND STLBAC

	C= 1.1 mF		C=0.7 mF	
Irradiance	RNBC	STLBAC	RNBC	STLBAC
1000 W/m^2	3.03 %	1.52 %	2.84 %	1.53 %
400 W/m^2	8.14 %	3.88 %	7.5 %	3.88 %

LAB/SIMULINK environment followed by experimentation in 2.5 kW GTPVS prototype. An Incremental Conductance (IC) MPPT algorithm calculates the V_{ref}. The STLBAC based PVVC is developed in pu. In simulation, the base value of F_{pv}, V_{pv}, and V_{ref} are considered as 6 A, 1000 V, and 1000 V respectively. In experimentation, the base value of F_{pv}, V_{pv}, and V_{ref} are considered as 10 A, 400 V, and 400 V respectively. The λ is chosen as 100. The maximum allowable V_{pv} tracking error (i.e., e) is considered as $\pm$ 1 V. STLBAC based PVVC gives adjustment of k automatically based on V_{pv} tracking error (i.e., e), and simultaneously settling of the V_{pv} at V_{ref} by maintaining the critically damped tracking response with the desired settling time. The efficacies of the proposed STLBAC are compared with RNBC [9]. Nominal parameters of GTPVS, used in simulation, are shown in Table. I.

A. Simulation verification

The PV modules voltage, current and power under different irradiance are tabulated in Table II. V_{mpp} is the PV module voltage at maximum PV power at current environmental condition. P_{mpp} and I_{mpp} are the respectively power and current of PV module when V_{pv} equals to V_{mpp}. The comparisons of V_{pv} tracking responses are shown in Fig. 3 while V_{ref} varies from 1000 V to 1005 V under both aged (i.e., C = 0.7 mF) and designed (i.e., C = 1.1 mF) DC-link capacitor. It is observed from Fig. 3(a) and Fig. 3(b) that the STLBAC provides smooth critically damped V_{pv}tracking responses with desired settling time under both designed and aged DC-link capacitor. But, overshoot is observed in V_{pv} tracking response obtained with RNBC. Further, maximum overshoot in V_{pv} tracking response, obtained with RNBC, varies with variation in capacitance of DC-link capacitor. Thus, STLBAC provides better V_{pv} tracking as compared with RNBC despite the uncertainties in C.

1) Performance under sudden change in irradiances: Now the efficacies of the STLBAC are discussed under sudden change in irradiance with designed and aged DC-link capacitor. The simulation starts with initial irradiance of 1000 W/m^2. Later, the irradiance changes to 400 W/m^2 at 2 sec. V_{ref} changes according to MPPT algorithm after 0.8 sec from initial value of 1010 V. The V_{pv} tracking characteristics under designed (i.e., C = 1.1 mF) and aged (i.e., C = 0.7 mF) DC-link capacitor are shown Fig. 4(a) and Fig. 4(b), obtained with respectively RNBC and STLBAC, under variation in irradiance. It is observed that MPPT operation is achieved by both RNBC and STLBAC as V_{pv} perturbs around the V_{mpp} in three steps [10]. However, from the zoomed view of V_{pv} tracking, as shown in Fig. 5(a) and Fig. 5(b), at 400 W/m^2 irradiance it is observed that voltage ripple in V_{pv} is more under RNBC as compared to STLBAC. Further, STLABC ables to maintain the critically damped V_{pv} tracking with 20 ms settling time.

The waveforms of grid currents (i.e., i_a) at irradiance of 400 W/m^2 are shown in Fig. 6(a) and Fig. 6(b) under RNBC and STLBAC respectively. It is observed that the grid current THD is more under RNBC as compared to STLBAC. The smooth V_{pv} tracking with less ripple improves the performance of GCC. As a result STLBAC provides improved grid current THDs as compared to RNBC. The comparisons in grid current THDs between RNBC and STLBAC are shown Table. III. From there it is observed that the THDs yielded by STLBAC in both high and low irradiance are well within the specified limit of IEEE 1547 (i.e., THD $<$ 5 %), whereas, THDs in low irradiance becomes more than 5 % with RNBC.

The behaviors of adaptation gain (k) under varying irradiance are shown in Fig. 7 for C = 1.1 mF and C = 0.7 mF. It is observed that the proposed self-tunning mechanism of adaptation gain is stable.

2) Performance under RL loading at PCC: Efficacies of STLBAC are verified under sudden loading at PPC by a Resistive Inductive (RL) load. A star connected RL load (2.5 kW, 2.5 kVAR) is connected at PCC at 0.75 sec. V_{ref} is maintained fixed at 1000 V in this study. The roles GTPVS are to generate the required reactive power of local load by maintaining the active power balancing between inverter and grid. Fig. 8(a) demonstrates the loading effect on V_{pv} tracking. It is observed from Fig. 8(a) that STLBAC enables V_{pv} to track the V_{ref} effectively. However, there is a dip in V_{pv} tracking due to sudden loading. STLBAC ables to settle the V_{pv} to V_{ref} within 24 ms after the loading.

The active and reactive power balancing are shown in Fig. 8(b) and Fig. 8(c) respectively. P_{inv} and Q_{inv} denote

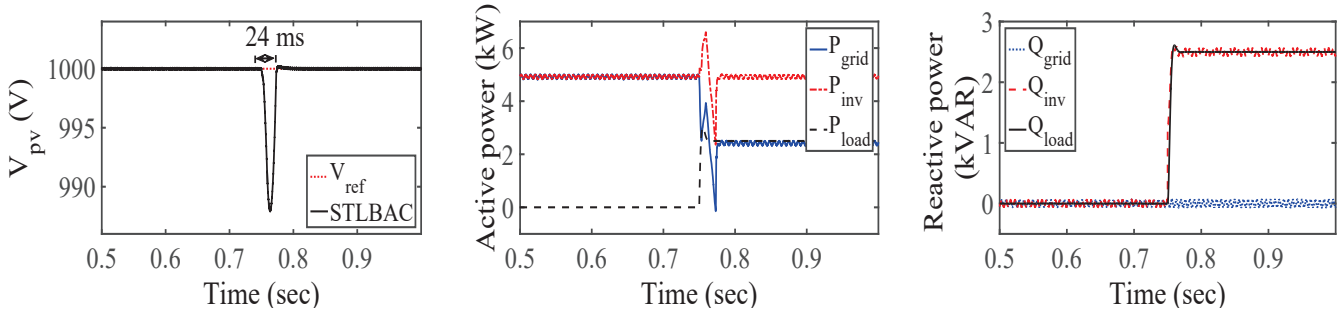

Fig. 8. Performance under sudden loading condition: (a) V_{pv} tracking, (b) active power balancing, and (c) reactive power balancing.

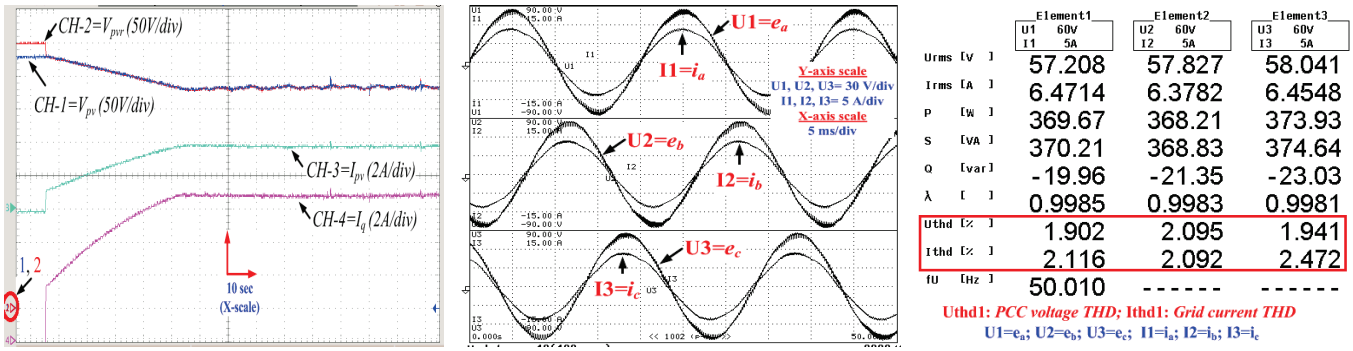

Fig. 9. Tracking performance of STLBAC.

respectively active and reactive power of inverter. Similarly, active power consumption by grid and load are denoted by respectively P_{grid} and P_{load}. Further, reactive power consumption by grid and load are denoted by respectively Q_{grid} and Q_{load}. It can be found from Fig. 8(b) and Fig. 8(c) that inverter injects the active power to the grid by maintaining the unity power factor as $P_{inv} = P_{grid}$, and $Q_{inv} = Q_{grid} \rightarrow 0$. Further after connection of local load at 0.75 sec, inverter full-fills the power demand by load (both active and reactive power), and injects the remaining 2.5 kW to the grid.

B. Experimental verification

Now the efficacy of the proposed STLBAC based PVVC is varified through the experimentation in 2.5 kW GTPVS prototype as described in [10]. A roof-top mounted solar plant (with power rating at STC as P_{mpp} = 2 kWp, V_{oc} = 400 V, V_{mpp} = 330.4 V, and I_{mpp} = 6.82 A) is used in experimentation. The various parameters of controller are chosen as f_{sw} = 10 kHz, T_{si} = 20 ms, T_{sv} = 300 ms, ΔV = 1 V, and T_{mppt} = 1 sec. The voltage of PCC is kept at 100 V through auto-transformer from 415 V (50 Hz) distribution grid. Fig. 9 shows the tracking performances of GTPVS. The waveforms of I_{pv}, I_q, V_{ref}, and V_{pv} are shown in Fig. 9(a). Initially V_{pv} at V_{oc}, and settles at V_{ref} after starting of controller. Later, due to MPPT operation V_{ref} decreases, and V_{pv} follows the V_{ref}. Finally, the V_{ref} and V_{pv} perturb around the V_{mpp} (i.e., 328 V). Also, I_q and I_{pv} gradually increase from zero to inject the extracted PV power to the grid as observed from Fig. 9(a).

The waveforms of different grid phase currents (i.e., i_a, i_b and i_c) and PCC phase voltages (i.e., e_a, e_b and e_c) are shown in Fig. 9(b). It is observed that GTPVS injects power to the grid with unity power factor as grid current and PCC voltage are in same phase. The different power qualty parameters such as grid-current THD (Ithd), PCC voltage THD (Uthd), reactive power (Q), active power (Q), and displacement factor (λ) are shown in Fig. 9(c). λ is found more than 0.998. The grid current THDs are found 2.116 %, 2.092 % and 2.472 % respectively for $a-phase$, $b-phase$ and $c-phase$. Thus, satisfies the IEEE-1547 grid code.

V. Conclusions

In this paper, a STLBAC based PV voltage controller is proposed for single stage three-phase GTPVS. Further, a PI controller based self tunning mechanism is employed to tune the adaptation gain of the proposed adaptive controller. The self tunning mechanism for adaptation gain is found to be working fine. The STLBAC is efficient to maintain the desired PV voltage critically damped tracking response with specified settling time. Further low PV voltage ripple is achieved with improved grid current quality as compared to RNBC. The simulation and experimental results indicate the efficacy of the proposed STLBAC in achieving better PV voltage tracking as compared to RNBC. The THDs of grid current are found below 5 % limit as specified by the grid code (IEEE-1547).

VI. Acknowledgment

The authors would like to thank DST Govt. of India for supporting the research vide no. DST/INT/Thai/P-12/2019.

References

[1] M. Bhunia and B. Subudhi, "Evaluation of aging effect on dynamics and performances of a grid connected pv system," *International Journal of Power and Energy Systems*, vol. 39, no. 2, 2019.

[2] N. Agarwal, A. Arya, M. W. Ahmad, and S. Anand, "Lifetime monitoring of electrolytic capacitor to maximize earnings from grid-feeding pv system," *IEEE Trans. Ind. Electron.*, vol. 63, no. 11, pp. 7049–7058, Nov 2016.

[3] S. Mukherjee, V. R. Chowdhury, P. Shamsi, and M. Ferdowsi, "Model reference adaptive control based estimation of equivalent resistance and reactance in grid-connected inverters," *IEEE Trans. Energy Convers.*, vol. 32, no. 4, pp. 1407–1417, Dec 2017.

[4] I. Hammoud, K. Morsy, M. Abdelrahem, and R. Kennel, "Efficient model predictive power control with online inductance estimation for photovoltaic inverters," *Electrical Engineering*, vol. 102, no. 2, pp. 549–562, Jun 2020.

[5] O. P. Pahari and B. Subudhi, "Integral sliding mode-improved adaptive mppt control scheme for suppressing grid current harmonics for pv system," *IET Renew. Power Gener.*, vol. 12, no. 16, pp. 1904–1914, 2018.

[6] N. Mahdian-Dehkordi, M. Namvar, H. Karimi, P. Piya, and M. Karimi-Ghartemani, "Nonlinear adaptive control of grid-connected three-phase inverters for renewable energy applications," *Int. J. Control*, vol. 90, no. 1, pp. 53–67, 2017.

[7] R. Kadri, J. P. Gaubert, and G. Champenois, "An improved maximum power point tracking for photovoltaic grid-connected inverter based on voltage-oriented control," *IEEE Trans. Ind. Electron*, vol. 58, no. 1, pp. 66–75, Jan 2011.

[8] A. Elkholy, F. Fahmy, A. A. El-Ela, A. E.-S. A. Nafeh, and S. Spea, "Experimental evaluation of 8kw grid-connected photovoltaic system in egypt," *Journal of Electrical Systems and Information Technology*, vol. 3, no. 2, pp. 217 – 229, 2016.

[9] T. Roy and M. Mahmud, "Active power control of three-phase grid-connected solar pv systems using a robust nonlinear adaptive backstepping approach," *Solar Energy*, vol. 153, pp. 64–76, 2017.

[10] M. Bhunia, B. Subudhi, and P. K. Ray, "A lyapunov-based adaptive voltage controller for a grid connected pv system," *IET Smart Grid*, vol. 4, no. 4, pp. 381–396.

[11] M. Bhunia and B. Subudhi, "Fpga based system integration scheme for a grid connected photovoltaic system," in *2018 15th IEEE India Council International Conference (INDICON)*, 2018, pp. 1–6.